Turkish Journal of Electrical Engineering & Computer Sciences

http://journals.tubitak.gov.tr/elektrik/

Research Article

Turk J Elec Eng & Comp Sci
(2014) 22: 874 – 892

doi:10.3906/elk-1205-80

Shuffled frog leaping algorithm optimization for AC–DC optimal power flow dispatch

Abolfazl RAHIMINEJAD, Arash ALIMARDANI, Behrooz VAHIDI*, Seyed Hossein HOSSEINIAN
Department of Electrical Engineering, Amirkabir University of Technology, Tehran, Iran

Received: 29.05.2012 • **Accepted:** 02.01.2013 • **Published Online:** 17.06.2014 • **Printed:** 16.07.2014

Abstract: In this paper, a simple-implemented and reliable AC–DC optimal power flow (OPF) is proposed. Although high-voltage direct current (HVDC) transmission lines are being increasingly used in power systems, new optimization algorithms such as evolutionary and memetic algorithms, which never stick in local minimum, so far have not been implemented in the AC–DC OPF problem. An evolutionary algorithm known as the shuffled frog leaping algorithm (SFLA) is proposed in this paper to solve the OPF dispatch in an AC–DC power system (including both high-voltage alternating current and HVDC transmission lines). The implementation of the AC–DC OPF with these kinds of methods is much simpler than that of traditional (numerical) algorithms. In order to prove the quality of the SFLA, the proposed method is applied to 2 case studies, including the Western System Coordinating Council 9-bus and IEEE 30-bus power systems, and compared with the conventional particle swarm optimization (PSO) algorithm and 3 of its modified versions, while the constraints are all satisfied. The results of comparison indicate that the SFLA is a reliable and fast optimization method with higher quality solutions among the other applied algorithms.

Key words: AC–DC optimal power flow, shuffled frog leaping algorithm, particle swarm optimization, HVDC transmission lines

1. Introduction

In recent decades, electric power systems have significantly increased around the world. Growing power consumption, long-distance transmission, submarine or underground transmission, and interconnection between countries or regions with different frequency power systems have led many countries to consider the high-voltage direct current (HVDC) transmission system as a solution to use the existing power transmission system more efficiently and satisfy the surge in energy demand. The economics of bulk power transmission by underground equipment is growing in favor of direct current [1]. Moreover, many developing countries have the problem of fundamental investment in transmission and distribution systems due to inadequate investment in the past. One solution to reduce the gap between the transmission capacity and power demand is employing HVDC transmission systems in the existing AC network to achieve an economic benefit from the investment [2].

Although the main reason for selecting HVDC transmission lines is often economic, there are some other reasons as well. HVDC may be the most feasible way to interconnect 2 asynchronous networks, reduce fault currents, employ long underground cable circuits, eliminate network congestion and distortion transmit restriction in interconnected systems, control the power line flow, and mitigate environmental concerns. In all of these applications, HVDC nicely complements the AC transmission system [3,4].

*Correspondence: vahidi@aut.ac.ir

Because of the mentioned reasons, HVDC transmission systems have been used in many countries around the world for different purposes since 1954 [5].

With the expansion of HVDC transmission systems in power networks, it is necessary to study the effect of these systems on power network operation. Researchers have provided various HVDC models for different purposes such as power flow studies [6–18].

Although many optimal power flow (OPF) and optimal reactive power flow studies have been performed on AC systems with various methods including traditional and evolutionary methods [19–28], little effort has been spent on AC–DC systems in which all of them use numerical methods for solving the problem [1,2,5,29–32]. On the other hand, the implementation of AC–DC OPF with numerical methods is difficult and complicated. Thus, in this paper, some evolutionary methods are chosen for solving AC–DC OPF dispatch and compared with each other. These evolutionary methods include the particle swarm optimization (PSO) algorithm, which was discussed in [33], and some of its modified versions and the SFLA, which is presented later in this paper.

Thus far, nonlinear equations of the AC–DC OPF problem have been solved using conventional methods such as the quadratic programming technique and Newton's method [5,30]. These classical optimization methods are limited to differentiable, convex, and continues algebraic objective functions and constraints and may depend on the specific objective function and/or constraints [34]. Furthermore, these methods need a lot of additional mathematical calculations and become more unreliable by increasing the complexity of the objective function. Moreover, the implementation of these methods for big objective functions with a lot of nonlinear constraints, such as OPF and AC–DC OPF, is very difficult. Recently, a new branch of optimization methods known as evolutionary algorithms was developed and employed in many engineering applications [35–37]. These algorithms do not require any specific initial guess and can deal with complex objective functions and constraints, and the implementation of these methods is very simple. However, to the best of the authors' knowledge, these optimization algorithms have not been applied in the AC–DC OPF problem.

In this paper, a new solution for the AC–DC OPF problem, known as the shuffled frog leaping algorithm (SFLA), is proposed. SFLA is a meta-heuristic optimization method based on observing and modeling the behavior of frogs. SFLA combines the benefits of genetic-based memetic algorithms (MAs) and the social behavior-based PSO algorithm [38,39]. This method is faster than the PSO method and its modified versions and has the best results among other methods discussed in this paper. Aside from the good results and high speed of this method in finding optimum answers, the implementation of this method to AC–DC OPF and even to any objective function is easier than numerical methods.

The rest of this paper is organized as follows: Section 2 describes the problem formulation and HVDC model in the OPF problem. Four versions of the PSO algorithm are explained briefly and the SFLA is presented in detail in Section 3. A case study is applied to the Western System Coordinating Council (WSCC) 9-bus and IEEE 30-bus power test systems in Section 4. Finally, Section 5 contains the conclusion.

2. Problem formulation

2.1. Optimal power flow

The OPF problem can be mathematically written as [30]:

$$Min \quad f(x), \tag{1}$$

$$S.T. \quad h(x) = 0, \tag{2}$$

$$g(x) \leq 0, \tag{3}$$

$$x_{min} \leq x \leq x_{\max}, \tag{4}$$

where $f(x)$ is the objective function that must be minimized. Various objective functions such as the fuel cost, active losses, voltage deviation, system stability, and control effort can be considered in the OPF problem. x is the vector of the state variables of the system. $h(x)$ consists of the equality constraint of the system and is always active during the optimization process [30]. $g(x)$ consists of inequality constraints (nonlinear constraints), such as the thermal limit of the lines, and active and reactive power generation. x_{max} and x_{min} are the upper and lower bounds of the state variable, respectively.

AC–DC systems consist of both the AC equipment and converters, which may include HVDC transmission systems. Hence, both AC and DC systems must be modeled in the AC–DC OPF problem.

2.2. AC system equations in load flow problem

Figure 1 represents a power system bus that includes a generator, load, shunt compensation, HVDC, and AC transmission line.

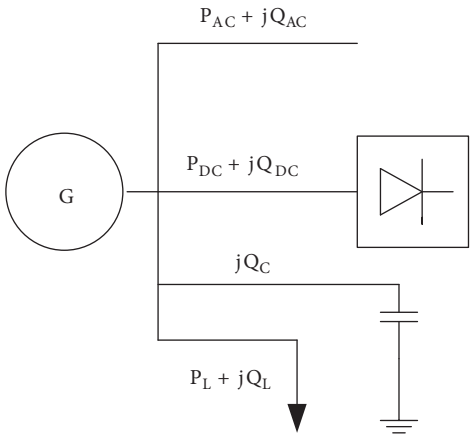

Figure 1. Bus system representation.

The injected active and reactive power in this bus can be expressed as follows:

$$P_i = P_G - P_L - P_{AC} - P_{DC}, \tag{5}$$

$$Q_i = Q_G + Q_C - Q_L - Q_{AC} - Q_{DC}. \tag{6}$$

For AC systems, active and reactive power injection in bus k can be written as:

$$P_k = \sum_{m}^{Nb} V_k V_m Y_{km} \cos(\delta_k - \delta_m - \theta_{km}), \tag{7}$$

$$Q_k = \sum_{m}^{Nb} V_k V_m Y_{km} \sin(\delta_k - \delta_m - \theta_{km}). \tag{8}$$

These nonlinear equations, which are known as power balance equations, are load flow equations and must be solved by iterative methods such as Newton–Raphson and Gauss–Seidel. By solving these equations, the voltage magnitude and angle, as well as the active and reactive power of the slack bus generator, are obtained.

The state variables in AC systems are V and δ, and constraints are applied to the voltage magnitude, and active and reactive power capacities of the generators and thermal limits of the transmission lines.

2.3. DC system equations in load flow problem

An equivalent circuit for the converter in bus k is shown in Figure 2.

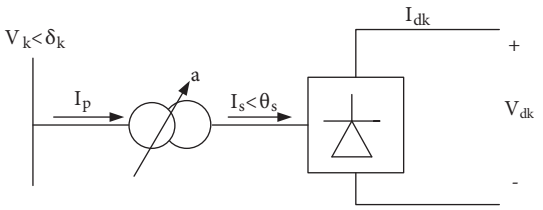

Figure 2. Equivalent circuit for the converter [30].

In this equivalent circuit, the angle of the converter's input current is considered 0. Variables are as follows [40]:

$V_k < \theta_k$: the voltage of the AC bus with respect to the DC bus as a reference bus (this means θ_k is the angle by which the fundamental converter's input current lags the V_k)

I_s, I_p: the fundamental current in the primary and secondary of the converter transformer

α: ignition angle of the converter

a: tap ratio of the converter transformer

V_d, I_d: DC voltage and DC current

The state variables for a converter are V_d, I_d, α, a, and θ_k. Since for an HVDC transmission line there are 2 converters, 10 state variables are required. However, I_d is common to both converters and consequently the number of state variables for each HVDC line reduces to 9. Thus, the set of state variables can be represented as follows:

$$X_{HVDC} = [V_{dr} V_{di} I_d a_r a_i \cos(\alpha) \cos(\gamma) \theta_r \theta_i]^T. \tag{9}$$

Index r is used to denote the rectifier operation and index i is used to denote the inverter operation of the converters. To linearize the equations and consequently improve the convergence, $cos(\alpha)$ and $cos(\gamma)$ are used as variables rather than α and γ [40].

To calculate these 9 variables, 9 independent equations are required. The rectifier's equations are summarized as follows [40]:

$$R_1^{'} = V_{dr} - k_1.a_r.V_{term\_r}.\cos(\varphi_r) = 0, \tag{10}$$

$$R_2^{'} = V_{dr} - \frac{3\sqrt{2}}{\pi} a_r.V_{term\_r}.\cos(\alpha) + \frac{3}{\pi} X_{Cr}.I_d = 0, \tag{11}$$

$$R_3^{'} = V_{dr} + V_{di} - R_{dc} I_d = 0, \tag{12}$$

$$R_4^{'} : \text{the first control's equation for rectifier}, \tag{13}$$

$$R_5^{'} : \text{the second control's equation for rectifier}. \tag{14}$$

k_1 is defined as follows:

$$k_1 = k\frac{3\sqrt{2}}{\pi}, \tag{15}$$

where k is used to consider the effect of the overlap and ripples in the DC current and the value of 0.995 is used in load flow studies [41].

The inverter's equations are summarized as follows [40]:

$$R_1^{''} = V_{di} - k_1.a_i.V_{term\_i}.\cos(\varphi_i) = 0, \tag{16}$$

$$R_2^{''} = V_{di} + \frac{3\sqrt{2}}{\pi}a_i.V_{term\_i}.\cos(\gamma) - \frac{3}{\pi}X_{Ci}.I_d = 0, \tag{17}$$

$$R_3^{''} = V_{di} + V_{dr} - R_{dc}I_d = 0, \tag{18}$$

$$R_4^{''} : \text{the first control's equation for inverter}, \tag{19}$$

$$R_5^{''} : \text{the second control's equation for inverter}. \tag{20}$$

These equations are explained in the Appendix. There are some controlling modes for each converter in the literature. In OPF studies, the controlling mode of the HVDC line can be considered fixed or as an optimization variable [30]. In this paper, these 2 cases are discussed and for the fixed controlling mode the controlling modes for the rectifier are a fixed current as $R_4^{'}$ and a controlling voltage limit as $R_5^{'}$, and for the inverter the controlling modes are a fixed voltage as $R_4^{''}$ and a fixed extinction angle as $R_5^{''}$ [17].

Hence, there are 10 equations in which equation $R_3^{'}$ is the same as equation $R_3^{''}$ and there are 9 independent equations that are used to calculate the 9 DC variables.

There are 2 methods for the AC–DC load flow. These 2 methods are known as the unified and sequential methods. In the unified method, all of the parameters are updated simultaneously in each iteration, while in the sequential method, the AC and DC equations are solved separately in each iteration. In this paper, the sequential method is employed due to its simple implementation and fast convergence [6–7,11–17]. Figure 3 shows the flowchart of the sequential AC–DC load flow.

The initial guesses for the AC system are:

The voltage amplitude of the PQ busses is considered as 1 pu and the voltage angle of all of the busses is considered 0.

For the DC system, the initial guesses are as follows:

The power factor of converters is usually considered as 0.9 [17,40]. From a network point of view, the rectifier consumes active power and the inverter generates it. Thus, the initial guesses can be considered as:

$$\theta_r \cong 25^0 and \theta_i \cong 155^0. \tag{21}$$

The ignition and extinction angles are usually assumed to be 150 and 21.50, respectively. These values are prepared for $5 < \alpha_{min} < 7$ and $15 < \gamma_{min} < 18$ [17,40]. The initial guess for the converter tap ratio is 1.

The other DC parameters can be determined according to these initial guesses. Using Eq. (10) and the specific values of V_{term-r}, θ_r, and a_r, the V_{dr} can be determined. By substituting V_{dr} in Eq. (11) and the specific value of the extinction angle of the inverter, V_{di} can be determined. I_d is calculated using Eq. (12) and by substituting V_{di} in Eq. (17), $\cos(\gamma)$ is obtained. Using Eqs. (22)–(25), P_d and Q_d can be calculated.

$$P_{dk} = V_k I_k \cos(\theta_k) \tag{22}$$

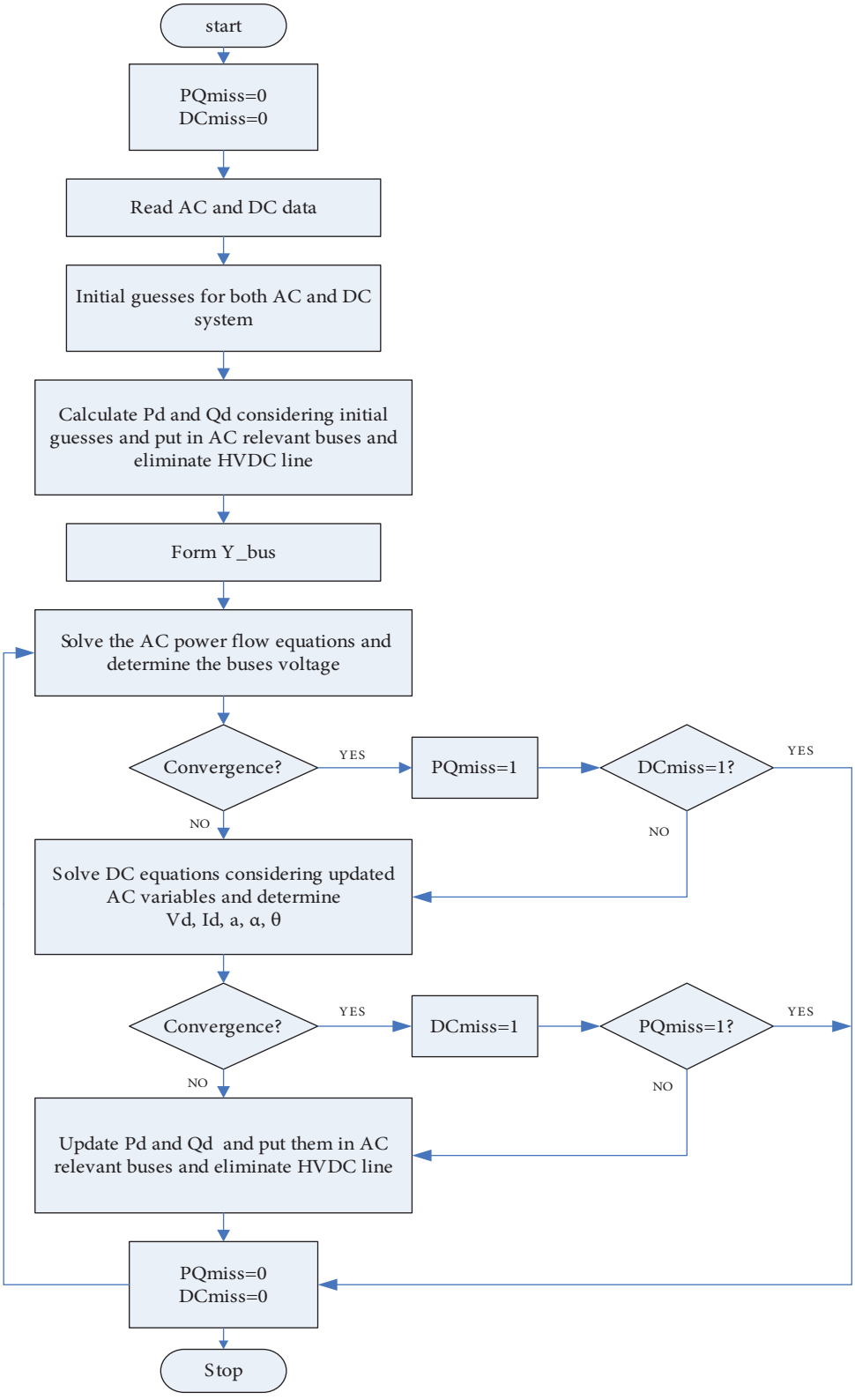

Figure 3. Flowchart of the sequential AC–DC load flow.

or

$$P_{dk} = V_{dk} I_{dk} \tag{23}$$

$$Q_{dk} = V_k I_k \sin(\theta_k) \tag{24}$$

or

$$Q_{dk} = P_{dk} \tan(\theta_k) \tag{25}$$

The constraints of the HVDC transmission line can be applied to the tap ratio of the converter transformer, ignition and extinction angle of the converters, DC voltage of the converters, DC current, and active power and reactive power of the converters.

2.4. HVDC model in OPF problem

To date, all AC–DC OPF research has used traditional methods, which have some problems such as: 1) the need for initial guesses; 2) additional mathematical calculations, such as the gradient differential; 3) dependence on the initial guesses and the shape of objective function; 4) sticking in local minimum; and 5) difficult implementation.

Due to the above reasons, in this paper, some evolutionary methods are proposed to solve the AC–DC OPF problem. Considering the AC–DC load flow, which was introduced in the previous section, implementation of the OPF with the SFLA is very simple. The iterative process for the AC–DC OPF is as follows:

Step 1: Generate randomly the population of the state variables in a defined range.

Step 2: Put each set of variables in the AC–DC load flow and calculate the bus voltage and power line flow.

Step 3: Check the constraints.

Step 4: Check the convergence criteria.

Step 5: Change the state variables to converge to the better results considering the evolutionary method.

In the first step, a population of variables is generated randomly in a defined range. In step 2, each set of variables is put in the load flow program. Some constraints, such as the reactive power generation limit and tap ratio limit, are checked in the load flow program. Other constraints, such as the power line flow limit and voltage amplitude limit are checked after convergence in the load flow. If there are any violations in these kinds of constraints, a big penalty coefficient is added to the objective function. The variables then change by the evolutionary method to improve the results. When the convergence criterion is satisfied, the AC–DC OPF is finished.

In the proposed method, no Lagrangian function is needed. There are no additional mathematical calculations or hessian matrix. The handling limits in both the AC system and DC system are very easy and do not need any definition of new variables. The results of this method are also better than traditional methods and more reliable.

3. SFLA

Before introducing the SFLA, the PSO algorithm and 3 of its modified versions are explained briefly.

PSO is a population-based stochastic search algorithm that was first introduced by Kennedy and Eberhart [42]. Since then, it has been greatly used to solve a wide range of optimization problems in different aspects [43,44]. The algorithm simulates the natural behavior of some animals such as insects or birds in finding food sources. Preceding the algorithm is the definition of a random population, which is called a swarm, and each member of this swarm is called a particle. Each particle in PSO flies through the search space and remembers the best position it has seen. All of the members of a swarm share their information about good positions and

dynamically adjust their own position and velocity based on these good positions. The velocity adjustment is based on the historical behaviors of the particles themselves as well as their neighbors. Hence, the particles tend to fly towards better and better search areas over the searching process. Mathematically, the particles are operated according to the following equation:

$$V_i^{(t+1)} = \omega \cdot V_i^{(t)} + c_1 \cdot rand_1(\cdot) \cdot \left(P_{best_i} - X_i^{(t)}\right) + c_2 \cdot rand_2(\cdot) \cdot \left(G_{best} - X_i^{(t)}\right), \tag{26}$$

$$X_i^{(t+1)} = X_i^{(t)} + V_i^{(t+1)}, \tag{27}$$

where t denotes the current iteration number; ω is called the inertia weight; c_1 and c_2 are the weighting factors of the stochastic acceleration terms, which pull each particle towards the P_{best_i} and G_{best} positions; $rand_1(\cdot)$ and $rand_2(\cdot)$ are 2 random functions in the range of [0,1]; $Pbest_i$ is the best previous experience of the ith particle that is recorded; and G_{best} is the best particle among the entire population.

In basic PSO or conventional PSO (C-PSO) the coefficients w, c_1, and c_2 are considered 1, 2, and 2, respectively. However, in some modified versions, different coefficients are used to obtain better results. One of these modified versions is called inertia constant PSO (IC-PSO) with 0.7298 for w and 2.01 for c_1 and c_2. The other version is linearly decreasing inertia PSO (LDI-PSO), in which the coefficients are defined as $w =$ 0.4–0.9 and $c_1 = c_2 = 2$. The other version of PSO, which is used in this paper, is Type 1 PSO (T1-PSO) and the coefficients for this version are defined as $w = 0.729$ and $c_1 = c_2 = 1.4944$.

3.1. Conventional SFLA

The SFLA was originally developed as a population-based metaheuristic to perform an informed heuristic search using mathematical functions to find a solution of a combinatorial optimization problem [45]. It combines the benefits of both the genetic-based MA and the social behavior-based PSO algorithm [46].

In SFLA, there is a population of possible solutions defined by a set of frogs that is divided into subgroups called memeplexes, each performing a local search. After a defined number of memetic evolution steps, ideas are passed among memeplexes in a shuffling process. The local search and the shuffling process continue until the defined convergence criteria are satisfied [46].

At first, an initial population of P frogs is created randomly within the feasible space. For an S variable problem, the ith frog is represented as $X_i = (x_{i1}, x_{i2}, \ldots, x_{iS})$. Next, the frogs are sorted in descending order according to their fitness. Next, the whole of population (P) is separated into m memeplexes, each containing n frogs. In this procedure, the 1st frog moves to the 1st memeplex, the 2nd frog moves to the 2nd memeplex, frog m moves to the mth memeplex, and frog $m + 1$ goes back to the 1st memeplex, etc.

Within each memeplex, the position of the frogs with the best and worst fitnesses is determined as X_b and X_w, respectively. Moreover, the position of the frog with the global best fitness is determined as X_g. Next, in each memeplex, a process is applied to improve only the frog with the worst fitness (not all frogs) in each cycle as follows:

$$D_i = Rand() \times (X_b - X_w), \tag{28}$$

$X_{w_{NEW}} = X_w + D_i$, (29) where *Rand()* is a random number between 0 and 1. If this process generates a better solution, the worst frog will be replaced. Otherwise, the calculations in Eqs. (28) and (29) are repeated with the replacement of *Xb* by *Xg*. If no improvement becomes possible in this case, then a new solution is randomly generated within the feasible space to replace the worst frog. Next, the calculations continue for a specific number of iterations [46]. Figure 4 shows the main idea of this algorithm.

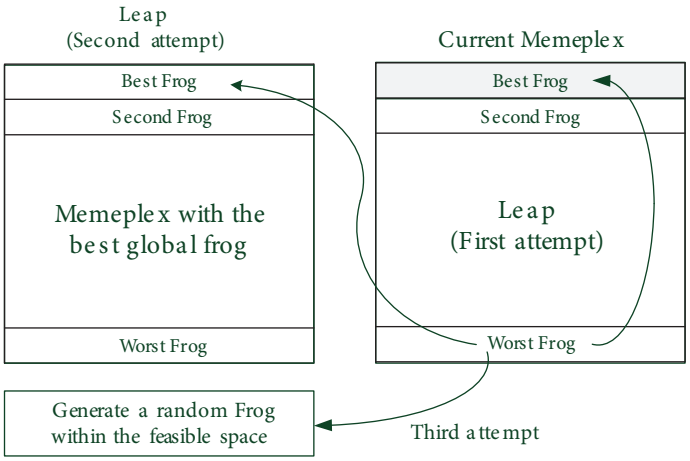

Figure 4. SFLA improvement attempts.

After a prespecified number of memetic evolutionary steps within each memeplex, to ensure global exploration, ideas passed within memeplexes are combined in the shuffling process [45]. The local search and the shuffling continue until the convergence criteria are satisfied. Figure 5 illustrates the SFLA.

3.2. Improvement of conventional the SFLA

In this section, the presented classic SFLA is improved. As Eqs. (28) and (29) represent, the worst frog tries to find a better place by jumping toward the best frog, but as the random operator is within 0 and 1, only the space between the 2 frogs is searched. However, as the space beyond the best frog (the other side of the best frog) might be a suitable place of solution, there should be a possibility so that the frog could search that area as well. Thus, the random operator is adjusted to rand (1, 1.75) in order to provide a chance to search the other side of the best frog, where 1.75 is chosen according to the authors' experiences in different problems.

The other difference of the improved (ISFLA) from the conventional one is that in the conventional SFLA, all of the elements of Xb-Xw in Eq. (28) are multiplied in the same random value. In the ISFLA, for each element of Xb-Xw, a random value is generated and multiplied in Eq. (28). It should be noted that the ISFLA will be SFLA in the results of this paper.

4. Case study

In this section, the OPF is studied on 2 test systems including the WSCC 9-bus and IEEE 30-bus [47] and compared with the conventional PSO algorithm and 3 of its modified versions, as the well-known popular evolutionary algorithm. The cost function of the generators for these systems is given in the appendix.

The AC–DC OPF has also been implemented for 2 cases:

Case 1: OPF for a fixed HVDC controlling mode

Case 2: OPF with optimization of the HVDC controlling mode, known as full AC–DC OPF.

4.1. Parameter setting

The evolutionary algorithms that are applied for comparison with the conventional SFLA are the C-PSO, IC-PSO, LDI-PSO, and T1-PSO [38,39]. The maximum number of iterations for all of the algorithms is set to 100. In the SFLA, the number of iterations for each memeplex is set to 8.

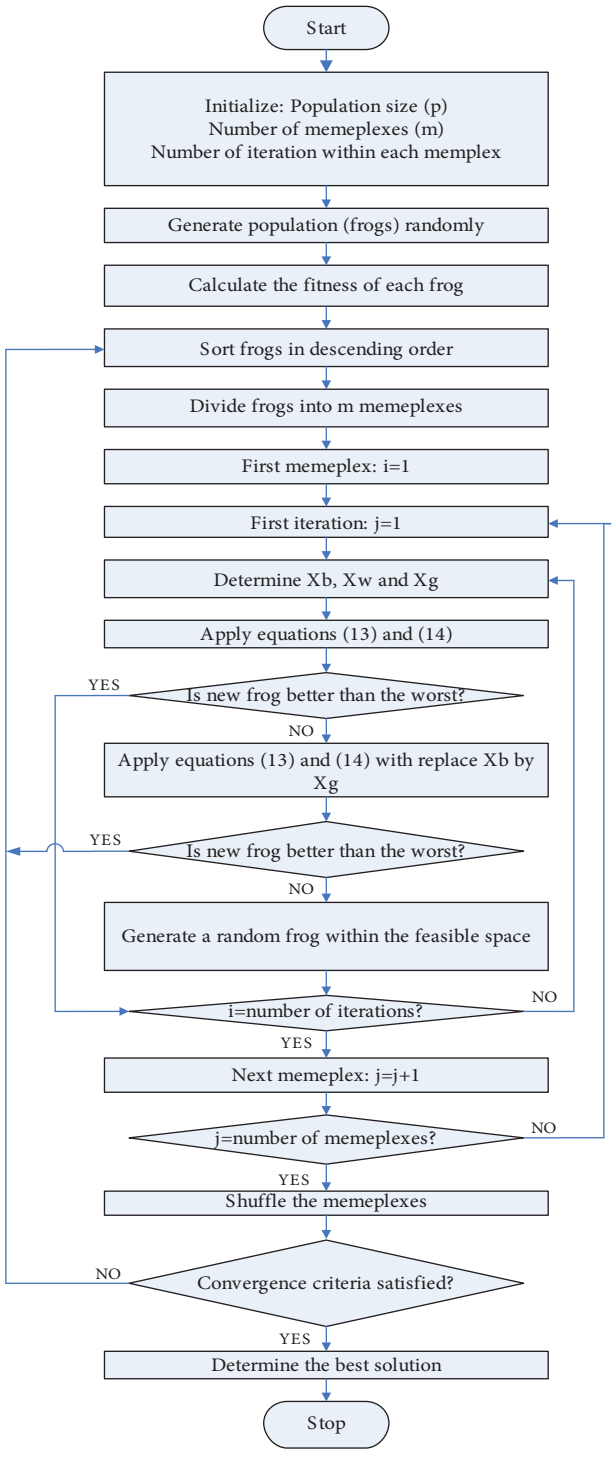

Figure 5. Flowchart of the SFLA.

For each algorithm, 20 independent trials are made. The population size (number of particles of different types of PSO), the number of memeplexes in the SFLA, and the number of frogs in each memeplex are, respectively, set as: 100, 7, and 15. All of the algorithms are implemented in MATLAB 7.6 and the simulation is run on a Pentium IV E5200 PC with 2 GB of RAM.

4.2. Case 1:

4.2.1. WSCC 9-bus power system

The WSCC 9-bus test system is modified for the incorporation of a HVDC link between buses 7 and 8, as shown in Figure 6.

The transmission line data for the WSCC 9-bus test system are listed on Table 1. For Case 1, the HVDC characteristic and fixed controlling modes are given in Table 2.

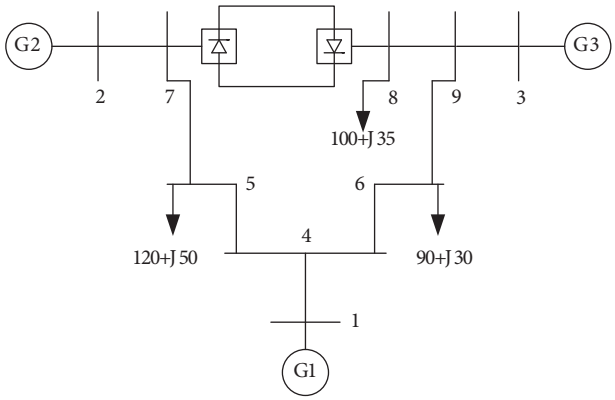

Figure 6. WSCC test system.

Table 1. Line data for the WSCC 9-bus test system.

From	To	R (pu)	X (pu)	B (pu)	Limit (MW)
1	4	0	0.0576	0	100
2	7	0	0.0625	0	200
3	9	0	0.0586	0	120
4	5	0.01	0.085	0.176	120
4	6	0.017	0.092	0.158	120
5	7	0.032	0.161	0.306	120
6	9	0.039	0.17	0.358	120
7	8	0.0085	0.072	0.149	120
8	9	0.0119	0.1008	0.209	120

Table 2. HVDC characteristics for the fixed controlling mode for the WSCC test system.

		Rectifier	Inverter
Commutation reactance (pu)		0.1	0.1
Bus number		7	8
DC-link resistance (pu)		0.00334	
Voltage (pu)	Max	1.25	Fixed 1.2
	Min	1	Fixed 1.2
Tap setting	Max	1.2	1.2
	Min	0.8	0.8
Angle (degree)	Max	15	25
	Min	5	15
	I (pu)	Fixed 0.45	

With regard to the randomness of the heuristic algorithms, the results of the methods change roughly around the optimum point in different runs. In order to prove if the algorithm is robust, many trials with

different initializations should be made. In this paper, 20 independent runs are implemented for each method and a comparison of the performance of the employed algorithms after these 20 independent runs is shown in Table 3. The mean value presented in Table 3 is the average value of all 20 answers and the best and worse values indicate the best and worse results among the 20 answers, which are obtained in 20 independent runs. As one can see, the best results for the mean, best, and worse answers are obtained by the SFLA. It also is the fastest method among these 5 algorithms.

Table 3. Statistic data for WSCC 9-bus test system.

Method	Fuel cost ($)			Time (s)			Solution (MW)		
	Mean	Best	Worse	Mean	Best	Worse	G1	G2	G3
C-PSO	6840.71	6840.61	6841.01	75.9	19.7	121.6	99.99	118.99	100
LDI-PSO	6840.56	6840.52	6840.61	99.3	74.4	131.1	99.99	120.48	98.47
IC-PSO	6840.57	6840.52	6840.61	90.7	31.5	121.8	99.99	120.75	98.19
TYPE-PSO	6840.58	6840.52	6840.61	77.1	51.9	100.2	99.99	120.49	98.46
SFLA	**6840.53**	**6840.52**	**6840.58**	**75.6**	**51.9**	**112.3**	**99.99**	**120.51**	**98.44**

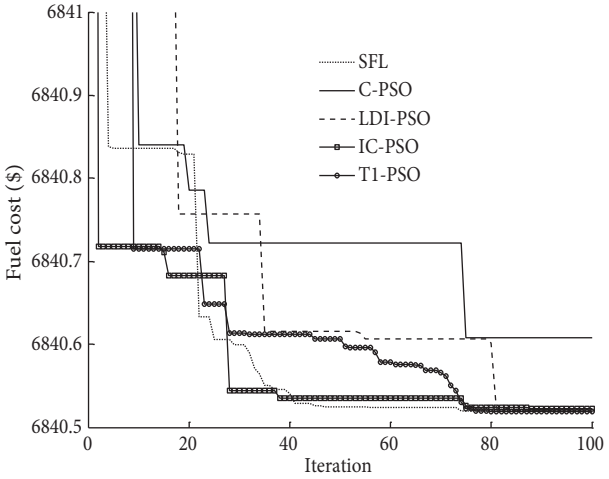

Figure 7. Convergence characteristics of different versions of PSO and the SFLA (with its improvement (ISFLA)) for AC–DC OPF of WSCC 9-bus power system.

The convergence characteristic of 5 methods for the OPF with a fixed controlling mode is shown in Figure 7. The behavior of different methods in finding the best point is shown by different line styles. Figure 7 illustrates that the SFLA not only gets the lowest points compared to the other methods but also reaches it at a lower iteration.

4.2.2. IEEE 30-bus power system

In the IEEE 30-bus test system, there are 2 HVDC links, which are connected between buses 2 and 6, and 8 and 28. The characteristics of the HVDC link in the IEEE 30-bus test system are listed in Table 4.

'HVDC-No' denotes the HVDC number, 'CR' denotes the commutation reactance, 'DC-R' denotes DC link resistance, and the controlling mode is the inverter voltage and DC current constant at a specific value.

Table 4. HVDC characteristics for the fixed controlling mode for the IEEE 30-bus test system.

HVDC No.		CR (pu)	DC-R (pu)	Voltage (pu)		Tap setting		Angle (degree)		I (pu)	Bus No.
				Max	Min	Max	Min	Max	Min		
1	Rec	0.146	0.00334	1.3	1	1.2	0.8	15	5	0.9	2
	Inv	0.0828		1.3		1.2	0.8	25	15		6
2	Rec	0.131	0.00334	1.3	0.9	1.2	0.8	15	5	0.7	8
	Inv	0.095		1.2		1.2	0.8	25	15		28

Table 5. Statistical data for the IEEE 30-bus test system.

Method	Fuel cost ($)			Time (s)		
	Mean	Best	Worse	Mean	Best	Worse
C-PSO	9917.96	9806.44	1026.59	345.7	71.8	505.8
LDI-PSO	9937.48	9803.34	1026.52	322.3	144	499.7
IC-PSO	9938.8	9803.31	1026.56	366.2	99.5	499.6
T1-PSO	9837.6	9803.37	9872.03	336.2	116	508.5
SFLA	**9830.95**	**9803.31**	**9871.83**	**267.3**	**41.1**	**536.7**

The statistical data for this system are given in Table 5, which depicts that in this system the SFLA has the best results and fast convergence.

4.3. Case 2

In Case 2, the controlling mode of the HVDC is considered as optimization variables next to the generation values. The HVDC data for the mentioned test systems are given in Tables 6 and 7. The PSO methods and SFLA are run 20 times and the mean value of the fuel cost and calculation time is given in Table 8. The convergence characteristic for the full AC–DC OPF (Case 2) is shown in Figure 8. The results in Table 5 and the behavior of the methods, which is shown in Figure 8, reveal that the best results with the fast convergence are achieved by the SFLA.

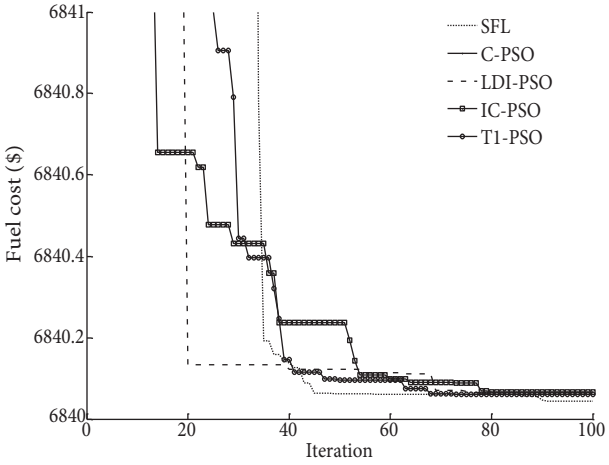

Figure 8. Convergence characteristics of different versions of PSO and the SFLA (with its improvement (ISFLA)) for the full AC–DC OPF of the WSCC 9-bus power system.

Table 6. HVDC characteristics for the full AC–DC OPF for the WSCC 9-bus power system.

Test system		HVDC characteristics			
		Voltage (pu)		I (pu)	
		Max	Min	Max	Min
WSCC	Rec	1.3	1	0.6	0.45
	Inv	1.3	1.1	0.6	0.45

Table 7. HVDC characteristics for the full AC–DC OPF for the IEEE 30-bus power system.

HVDC number		HVDC characteristics			
		Voltage (pu)		I (pu)	
		Max	Min	Max	Min
HVDC 1	Rec	1.3	1	0.6	0.45
	Inv	1.3	1.1	0.6	0.45
HVDC 2	Rec	1.3	1	0.6	0.2
	Inv	1.3	1	0.6	0.2

Table 8. Mean values for the test systems for the full AC–DC OPF.

Method	WSCC		IEEE 30	
	Fuel cost ($)	Time (s)	Fuel cost ($)	Time (s)
C-PSO	6850.19	78.00	9824.7	366.3
LDI-PSO	6841.34	95.17	9898.7	341.5
IC-PSO	6840.64	102.9	9888.4	315.9
T1-PSO	6842.19	81.85	9786.7	360.7
SFLA	**6840.44**	**78.03**	**9782.1**	**268.2**

5. Conclusion

An evolutionary algorithm optimization approach known as the SFLA is presented, improved, and applied in the AC–DC OPF problem to determine the optimal generation values in 2 case studies. The simple implementation, high quality results, and high speed in finding the optimum results are the main reasons for choosing the SFLA for solving the AC–DC OPF problem. To compare the performances of the SFLA with 4 versions of the PSO algorithm, the AC–DC OPF is applied to 2 different test systems (WSCC 9-bus and IEEE 30-bus power systems). The AC–DC OPF is run in 2 strategies. At first the HVDC parameters are considered fixed and in the second strategy the HVDC parameters are optimized during the optimization proceeding. Tables 3, 5, and 8 reveal that the SFLA not only has the best results, but is also the fastest method. The behavior of different methods during the optimization process is shown in Figures 7 and 8, where the high quality results of the SFLA with respect to the other methods are also shown. The main contributions of this paper are:

1. Implementation of evolutionary algorithms in the AC–DC–OPF because of their reliability and simple implementation.

2. Introducing and improving a rather recent optimization algorithm known as the SFLA.

3. Performing a comparison to show the override of the SFLA in competition with 4 versions of the PSO algorithm. Moreover, the SFLA's high quality performance is demonstrated.

Appendix

The Tables A.1 and A.2 show the generation data of the WSCC 9-bus and IEEE 30-bus test systems, respectively.

For the calculation of 9 variables in the HVDC lines, 9 independent equations are needed. Each converter has 5 equations and in total there are 10 equations for an HVDC transmission line. Regarding a common equation between 2 converters in each HVDC line, there are 9 independent equations that can calculate the 9 variables. The equations for each converter are as follows:

The relation between the DC and AC voltages of the bus to which the converter is connected can be shown as follows:

$$V_d^{P.U} = \frac{3\sqrt{2}}{\pi} a.V_{term}.\cos(\alpha) - \frac{3}{\pi} X_{eq}^{P.U}.I_d^{P.U}.$$

Considering the lossless transformer, the following equation illustrates the exchange power of the converters:

$$V_d.I_d = \sqrt{3}.V_{term}.I_p.\cos(\phi).$$

On the other hand, the primary current of transformer relates to the DC current as follows:

$$I_p = k.a.\frac{\sqrt{6}}{\pi} I_d.$$

From these 2 foregoing equations, it can be written:

$$V_d = k\frac{3\sqrt{2}}{\pi} a.V_{term}.\cos(\phi).$$

The following equation is obtained using KVL in the HVDC line:

$$V_{dr} + V_{di} - R_{dc}I_d = 0$$

Thus, to date, there are 3 independent equations for each converter and 2 more equations are needed. These 2 equations are obtained from the controlling mode of converters. The converter controlling mode for the HVDC lines are presented below:

Fixed tap ratio in the rectifier	$a_r - a_r^{sp} = 0$
Fixed tap ratio in the inverter	$a_i - a_i^{sp} = 0$
Fixed DC current	$I_d - I_d^{sp} = 0$
Fixed DC voltage in the rectifier	$V_{dr} - V_{dr}^{sp} = 0$
Fixed DC voltage in the inverter	$V_{di} - V_{di}^{sp} = 0$
Fixed active power flow in the rectifier	$V_{dr}.I_d - P_r^{sp} = 0$
Fixed active power flow in the inverter	$V_{di}.I_d - P_i^{sp} = 0$
Fixed ignition angle	$\cos(\alpha) - \cos(\alpha_{\min}) = 0$
Fixed extinction angle	$\cos(\gamma) - \cos(\gamma_{\min}) = 0$
controlling voltage limit in the rectifier	$V_{dr} - 0.97\frac{3\sqrt{2}}{\pi} a_r V_{term\_r}\cos(\alpha_{\min}) + 0.97\frac{3}{\pi} X_{Cr} I_d = 0$
controlling voltage limit in the inverter	$V_{di} + 0.97\frac{3\sqrt{2}}{\pi} a_i V_{term\_i}\cos(\gamma_{\min}) - 0.97\frac{3}{\pi} X_{Ci} I_d = 0$
Fixed reactive power flow in the rectifier	$k_1 a_r V_{term\_r} I_d \sin(\phi_r) - Q_r^{sp} = 0$
Fixed reactive power flow in the inverter	$k_1 a_i V_{term\_i} I_d \sin(\phi_i) - Q_i^{sp} = 0$

Table A1. Cost function of the generators for the WSCC 9-bus test system.

Generator	α	β	γ	Bus No.	Pmax (MW)	Pmin	Qmax (MVAR)	Qmin (MVAR)
G1	0.01	18	50	1	135	0	50	–50
G2	0.014	20.4	50	2	200	0	50	–40
G3	0.02	19.3	85	3	100	0	50	–50

Table A2. Cost function of the generators for the IEEE 30-bus test system.

Generator	α	β	γ	Bus No.	Pmax (MW)	Pmin (MW)	Qmax (MVAR)	Qmin (MVAR)
G1	0.0043	20	47	1	100	0	20	0
G2	0.01	40	50	3	80	0	50	–40
G3	0.01	40	85	5	85	10	60	–20
G4	0.01	40	58	11	110	20	24	–60
G5	0.02	20	35	13	65	0	24	–60
G6	0.014	45	50	24	90	10	20	0

Nomenclature

HVDC	High-voltage direct current
HVAC	High-voltage alternative current
OPF	Optimal power flow
SFLA	Shuffled frog leaping algorithm
PSO	Particle swarm optimization
MA	Memetic algorithms
subscripts AC	AC parameters
subscripts DC	DC parameters
subscripts G	Generation
subscripts L	Load
subscripts C	Compensation
$\bar{X}$	State variables
$\bar{U}$	Control variables
P	Active power generation
Q	Reactive power generation
V	Terminal voltage magnitude
δ	Terminal voltage angle
I	Line current
g_k	Conductance of the kth transmission line
Y_{km}	Magnitude of the admittance between buses k and m
θ_{km}	Angle of the admittance between buses k and m
N_b	Number of buses
N_{pv}	Number of P.V. buses
α_k	Ignition angle of rectifier
γ	Extinction angle of inverter
r_{ck}	Commutation resistance
a_k	Converter transformer tap setting
F	Objective function
h(x)	Equality constraint
g(x)	Inequality constraint
μ	Membership function of the optimal decision function
Rand(a,b)	The function producing random numbers between a and b

References

[1] H. Ambriz-Pérez, E. Acha, C.R. Fuerte-Esquivel, "High voltage direct current modelling in optimal power flows", International Journal of Electrical Power & Energy Systems, Vol. 30, pp. 157–168, 2008.

[2] S.B. Warkad, M.K. Khedkar, G.M. Dhole, "Optimal electricity nodal price behavior: a study in Indian electricity market", Journal of Theoretical and Applied Information Technology, Vol. 5, pp. 734–744, 2009.

[3] M.P. Bahrman, B.K. Johnson, "The ABCs of HVDC transmission technologies, an overview of high voltage direct current systems and applications", IEEE Power & Energy Magazine, Vol. 5, pp. 32–44, 2007.

[4] H. Latorre, M. Ghandhari, "Improvement of power system stability by using a VSC-HVDC", International Journal of Electrical Power & Energy Systems, Vol. 33, pp. 332–339, 2011.

[5] J. Yu, W. Yan, W. Li, L. Wen, "Quadratic models of AC-DC power flow and optimal reactive power flow with HVDC and UPFC controls", International Journal of Electrical Power & Energy Systems, Vol. 78, pp. 157–168, 2008.

[6] H. Sato, J. Arrillaga, "Improved load-flow techniques for integrated a.c.–d.c. systems", Proceedings of the Institution of Electrical Engineers, Vol. 116, pp. 525–532, 1969.

[7] J. Reeve, G. Fahmy, B. Stott, "Versatile load flow method for multiterminal HVDC systems", IEEE Transactions on Power Apparatus Systems, Vol. 96, pp. 925–933, 1977.

[8] H. Fudeh, M.N. Ong, "A simple and efficient AC–DC load-flow method for multiterminal DC systems", IEEE Transactions on Power Apparatus Systems, Vol. 100, pp. 4389–4396, 1981.

[9] C.M. Ong, H. Fudeh, "AC power flow control with a multiterminal DC systems", IEEE Transactions on Power Apparatus Systems, Vol. 100, pp. 4686–4691, 1981.

[10] B. Stott, "Load flow for a.c. and integrated a.c.–d.c. systems", PhD Dissertation, Department of Electrical Engineering, University of Manchester; Manchester, U.K, 1971.

[11] G.B. Sheble, G.T. Heydt, "Power flow studies for systems with HVDC Transmission", Proceedings of the 9th IEEE Power Industry Computer Applications Conference, pp. 223–228, 1975.

[12] D.A. Braunagel, L.A. Kraft, J.L. Whysong, "Inclusion of DC converter and transmission equations directly in a Newton power flow", IEEE Transactions on Power Apparatus Systems, Vol. 95, pp. 76–88, 1976.

[13] J. Arrillaga, P. Bodger, "Integration of h.v.d.c. links with fast decoupled load flow solutions", Proceedings of the Institution of Electrical Engineers, Vol. 124, pp. 463–468, 1977.

[14] J. Arrillaga, P. Bodger, "A.C.–D.C. load flows with realistic representation of the convertor plant", Proceedings of the Institution of Electrical Engineers, Vol. 125, pp. 41–46, 1978.

[15] M.M. El-Marsafawy, R.M. Mathur, "A new, fast technique for load-flow solution of integrated multi-terminal DC/AC systems", IEEE Transactions on Power Apparatus Systems, Vol. 99, pp. 246–255, 1980.

[16] G. Fahmy, J. Reeve, B. Stott, "Load flow in multiterminal HVDC systems", GIGRE, Johannesburg, pp. 17–75(SC) 08, 1975.

[17] G.B. Gharehpatian, "AC-DC load flow", MS Thesis, Department of Electrical Engineering, Amirkabir University of Technology, Tehran, Iran, 1990.

[18] O. Alizadeh Mousavi, M.J. Sanjari, G.B. Gharehpetian, R.A. Naghizadeh, "A simple and unified method to model HVDC links and FACTS devices in DC load flow", Simulation, Vol. 85, pp. 101–109, 2009.

[19] C.H. Lin, S.Y. Lin, "A new dual-type method used in solving optimal power flow problems", IEEE Transactions on Power Systems, Vol. 12, pp. 1667–1675, 1997.

[20] H. Wei, H. Sasaki, J. Kubokawa, R. Yokoyama, "An interior point nonlinear programming for optimal power flow problems with a novel data structure", IEEE Transactions on Power Systems, Vol. 13, pp. 870–877, 1998.

[21] G. Tognola, R. Bacher, "Unlimited point algorithm for OPF problems", IEEE Transactions on Power Systems, Vol. 14, pp. 1046–1054, 1999.

[22] R.A. Jabr, "Optimal power flow using an extended conic quadratic formulation", IEEE Transactions on Power Systems, Vol. 23, pp. 1000–1008, 2008.

[23] W.J. Tang, M.S. Li, Q.H. Wu, J.R. Saunders, "Bacterial foraging algorithm for optimal power flow in dynamic environments", IEEE Transactions on Circuits and Systems, Vol. 55, pp. 2433–2442, 2008.

[24] M. Varadarajan, K.S. Swarup, "Solving multi-objective optimal power flow using differential evolution", IET Generation, Transmission & Distribution, Vol. 2, pp. 720–730, 2008.

[25] B. Mahdad, K. Srairi, T. Bouktir, "Optimal power flow for large-scale power system with shunt FACTS using efficient parallel GA", 14th IEEE Mediterranean Electrotechnical Conference, Vol. 32, pp. 507–517, 2010.

[26] S. Sivasubramani, K.S. Swarup, "Multi-objective harmony search algorithm for optimal power flow problem", International Journal of Electrical Power & Energy Systems, Vol. 33, pp. 745–752, 2011.

[27] M. Sailaja Kumari, S. Maheswarapu, "Enhanced genetic algorithm based computation technique for multi-objective optimal power flow solution", International Journal of Electrical Power & Energy Systems, Vol. 32, pp. 736–742, 2010.

[28] H.R. Cai, C.Y. Chung, K.P. Wong, "Application of differential evolution algorithm for transient stability constrained optimal power flow", IEEE Transactions on Power Systems, Vol. 23, pp. 719–728, 2008.

[29] U. De Martinis, F. Gagliardi, A. Losi, V. Mangoni, F. Rossi, "Optimal load flow for electrical power systems with multiterminal HVDC links", IET Proceedings – Generation, Transmission, & Distribution, Vol. 137, pp. 139–145, 1990.

[30] C.N. Lu, S.S. Chen, C.M. Ong, "The incorporation of HVDC equations in optimal power flow methods using sequential quadratic programming techniques", IEEE Transactions on Power Apparatus Systems, Vol. 3, pp. 1005–1011, 1988.

[31] D. Thukaram, L. Jenkins, K. Visakha, "Optimum allocation of reactive power for voltage stability improvement in AC–DC power systems", IET Proceedings – Generation, Transmission, & Distribution, Vol. 153, pp. 237–246, 2006.

[32] A. Pizano-Martinez, C.R. Fuerte-Esquivel, H. Ambriz-Pérez, E. Acha, "Modeling of VSC-based HVDC systems for a Newton-Raphson OPF algorithm", IEEE Transactions on Power Systems, Vol. 22, pp. 1794–1803, 2007.

[33] A.M. El-Zonkoly, "Optimal placement of multi-distributed generation units including different load models using particle swarm optimization", International Journal of Electrical Power & Energy Systems, Vol. 1, pp. 50–59, 2011.

[34] J.A. Momoh, M.E. El-Hawary, R. Adapa, "A review of selected optimal power flow literature to 1993. II. Newton, linear programming and interior point methods", IEEE Transactions on Power Systems, Vol. 14, pp. 105–111, 1999.

[35] A.E. Eiben, S.K. Smit, "Parameter tuning for configuring and analyzing evolutionary algorithms", International Journal of Electrical Power & Energy Systems, Vol. 1, pp 19–31, 2011.

[36] L.D. Santos Coelho, C.S. Lee, "Solving economic load dispatch problems in power systems using chaotic and Gaussian particle swarm optimization approaches", International Journal of Electrical Power & Energy Systems, Vol. 30, pp. 297–307, 2008.

[37] J. Derrac, S. García, D. Molina, F. Herrera, "A practical tutorial on the use of nonparametric statistical tests as a methodology for comparing evolutionary and swarm intelligence algorithms", International Journal of Electrical Power & Energy Systems, Vol. 1, pp. 3–18, 2011.

[38] Y.D. Valle, G.K. Venayagamoorthy, S. Mohagheghi, J. Hernandez, R.G. Harley, "Particle swarm optimization: basic concepts, variants and applications in power systems", IEEE Transactions on Evolutionary Computation, Vol. 12, pp. 171–195, 2008.

[39] Y. Shi, R. Eberhart, "A modified particle swarm optimizer", IEEE World Congress Computational Intelligence, IEEE International Conference on Evolutionary Computation Proceedings, pp. 69–73, 1998.

[40] J. Arrillag, B. Smith, AC-DC Power System Analysis, London, UK, The Institution of Electrical Engineers, 1998, ch. 3.

[41] J. Arrillaga, C.P. Arnold, B.J. Harker, Computer Modeling of Electrical Power System, The University of Michigan, Wiley, 1983, ch. 4.

[42] J. Kennedy, R.C. Eberhart, "Particle swarm optimization", Proceedings of International Conference on Neural Networks, Vol. 4, pp. 1942–1948, 1995.

[43] T. Niknam, H. Zeinoddini-Meymand, M. Nayeripour, "A practical algorithm for optimal operation management of distribution network including fuel cell power plants renewable energy", International Journal of Renewable Energy, Vol. 35, pp. 1696–1714, 2010.

[44] V. Miranda, N. Fonseca, "EPSO-evolutionary particle swarm optimization, a new algorithm with applications in power systems", IEEE/PES Transmission and Distribution Conference and Exhibition: Asia Pacific, Vol. 2, pp. 745–750, 2002.

[45] B. Amiri, M. Fathian, A. Maroosi, "Application of shuffled frog-leaping algorithm on clustering", International Journal of Advanced Manufacturing Technology, Vol. 45, pp. 199–209, 2009.

[46] E. Elbeltagi, T. Hegazy, D. Grierson, "Comparison among five evolutionary-based optimization algorithms", International Journal of Advanced Engineering Informatics, Vol. 19, pp. 43–53, 2005.

[47] R. Christie, Power Systems Test Case Archive (The IEEE 30-Bus Test System), [Online]. Last Access: Oct. 2012, Available at: http://www.ee.washington.edu/research/pstca/pf30/pg_tca30bus.htm, 1993.